Journal of Medicinal Chemistry

Article

pubs.acs.org/jmc

Structure-Based Design of β5c Selective Inhibitors of Human Constitutive Proteasomes

Bo-Tao Xin,[†] Gerjan de Bruin,[†] Eva M. Huber,[‡] Andrej Besse,[∥] Bogdan I. Florea,[†] Dmitri V. Filippov,[†] Gijsbert A. van der Marel,[†] Alexei F. Kisselev,[§] Mario van der Stelt,[†] Christoph Driessen,[∥] Michael Groll,[‡] and Herman S. Overkleeft*[,†]

[†]Gorlaeus Laboratories, Leiden Institute of Chemistry, Einsteinweg 55, 2333 CC Leiden, The Netherlands

[‡]Center for Integrated Protein Science at the Department Chemie, Lehrstuhl für Biochemie, Technische Universität München, 85748 Garching, Germany

[§]Department of Pharmacology and Toxicology and Norris Cotton Cancer Center, Geisel Cancer School of Medicine at Dartmouth, 1 Medical Center Drive HB7936, Lebanon, New Hampshire 03756, United States

[∥]Department of Hematology and Oncology, Kantonsspital St. Gallen, 9007 St. Gallen, Switzerland

Supporting Information

ABSTRACT: This work reports the development of highly potent and selective inhibitors of the β5c catalytic activity of human constitutive proteasomes. The work describes the design principles, large hydrophobic P3 residue and small hydrophobic P1 residue, that led to the synthesis of a panel of peptide epoxyketones; their evaluation and the selection of the most promising compounds for further analyses. Structure−activity relationships detail how in a logical order the β1c/i, β2c/i, and β5i activities became resistant to inhibition as compounds were diversified stepwise. The most effective compounds were obtained as a mixture of *cis*- and *trans*-biscyclohexyl isomers, and enantioselective synthesis resolved this issue. Studies on yeast proteasome structures complexed with some of the compounds provide a rationale for the potency and specificity. Substitution of the N-terminus in the most potent compound for a more soluble equivalent led to a cell-permeable molecule that selectively and efficiently blocks β5c in cells expressing both constitutive proteasomes and immunoproteasomes.

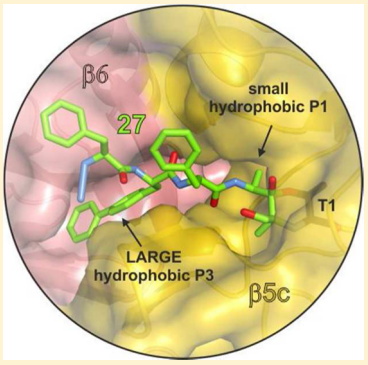

INTRODUCTION

The 20S proteasome core particle (CP) is the major cytosolic and nuclear protein degradation machinery in eukaryotes.[1] In vertebrates, three distinct CPs exist that differ in their tissue distribution, active site composition, substrate preferences, and in the signatures of the oligopeptide pools they produce. Constitutive proteasome core particles (cCPs), expressed in all mammalian tissues, contain β1c, β2c, and β5c catalytic subunits, with β1c cleaving preferentially after acidic residues, β2c after basic residues, and β5c after hydrophobic residues.[2] Hematopoietic cells constitutively express immunoproteasome core particles (iCPs), and other tissues may do so in an interferon-γ (INF-γ)-inducible manner.[3] In the iCP, β1c, β2c, and β5c are substituted by β1i (LMP2), β2i (MECL-1), and β5i (LMP7), respectively. The substrate preferences of iCPs differ from those of cCPs, most prominently in the respective β1 subunits: whereas β1c accepts both acidic (Asp) and hydrophobic (Leu) residues, β1i has evolved to cleave preferentially after hydrophobic residues.[4] As a consequence, iCP expressing cells produce oligopeptide pools in which basic and hydrophobic C-terminal residues are prevalent−oligopeptides that may bind well to major histocompatibility complex class I (MHCI) molecules.[5] For this reason, iCPs are thought to have evolved to enhance the peptide repertoire for MHCI-mediated antigen presentation; however, cCPs also make a significant contribution to the production of MHCI peptides. Cortical thymic epithelial cells that mediate positive $CD8^+$ T cell selection finally express thymoproteasome core particles (tCPs), essentially iCP particles in which β5i is substituted for β5t with an apparent loss of bias for cleavage after hydrophobic amino acid residues.[6] In total, vertebrate tissue may express up to seven catalytic activities, distributed over three distinct 20S core particles. Hybrid CPs composed of both constitutive proteasome and immunoproteasome catalytic activities exist as well[7] and may yield oligopeptide pools distinct from those produced by pure cCPs or iCPs.

Compounds able to selectively inhibit a single catalytic site of the CP are indispensable tools to study proteasome activity in the context of global protein turnover, to determine substrate preferences, and to establish the role of the individual activities in MHCI antigen processing. Moreover, proteasomes are the primary target of clinical drugs such as bortezomib,[8] carfilzomib,[9] and ixazomib[10] (with more clinical candidates in various stages of development) for the treatment of multiple myeloma and mantle cell lymphoma. All these compounds

Received: May 10, 2016
Published: July 20, 2016

DOI: 10.1021/acs.jmedchem.6b00705
J. Med. Chem. 2016, 59, 7177−7187

block several catalytic subunits of both cCPs and iCPs, thereby causing strong cytotoxicity. Subunit-selective inhibitors could be used to establish the optimal combination of catalytic activities both with respect to drug efficacy and (limited) side effects. Selective proteasome inhibitors have been the subject of extensive studies in recent years in several research groups both in academia and industry.[11] We recently reported[12] the development of an activity-based protein profiling (ABPP) assay that allows inspection of β1c/β1i, β2c/β2i, and β5c/β5i activities in a single experiment. With these probes, cCP and iCP subunits, which are expressed simultaneously by human cell lines and primary tumor tissues, can be resolved and visualized by SDS−PAGE. Together with the ABPP assay, we disclosed a set of inhibitors selective for each of the six catalytic activities of human cCPs and iCPs, including **52**, selective for β5i, and **29**, selective for β5c (Figure 1). The development of

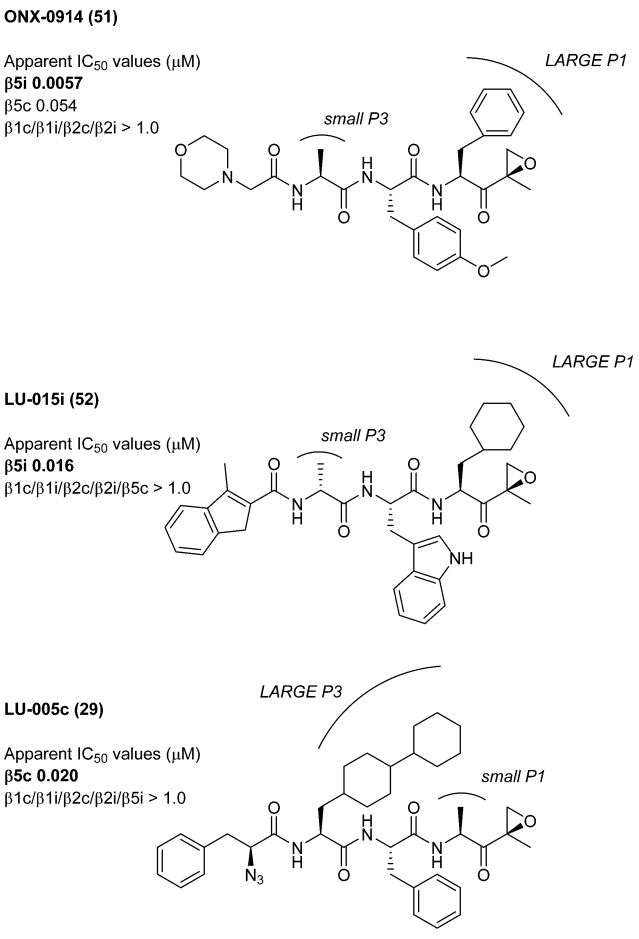

Figure 1. Structures and activities of the β5i-selective inhibitor ONX-0914 (**51**); the β5i-selective inhibitor LU-015i (**52**); and the β5c-selective inhibitor LU-005c (**29**).

52 was subject of an earlier report[13] from our laboratories. Here, we describe our results on the development of β5c-selective inhibitors. We show how screening of a focused library followed by modulating compound solubility led to the identification of **29**. Furthermore, we provide routes of synthesis toward enantiopure analogues of **29** with respect to the bis-cyclohexyl moiety at P3. A crystal structure of yeast CP complexed with one of our β5c specific inhibitors gives detailed insights into the mode of action and binding at the molecular level.

RESULTS

Our previous work[13] on the development of **52** started with perusal of the crystal structures of murine cCP and iCP.[14] The complex structures bound to the β5i inhibitor **51** (Figure 1) revealed that the S1 pocket of β5i was more suited to accommodate large hydrophobic residues than the corresponding S1 site of β5c and that the S3 pocket in β5i was due to Ser27 less spacious than the β5c counterpart (Figure 2).[14] On

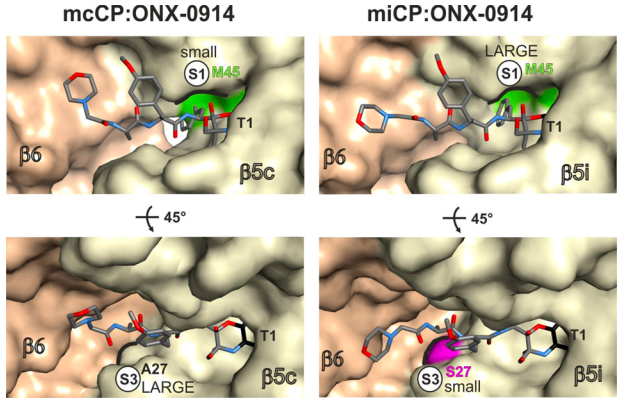

Figure 2. Crystal structures of the mouse cCP and iCP either without (PDB code 3UNE for mouse cCP and 3UNH for mouse iCP) or in complex with **51** (ONX-0914, PDB code 3UNB for mouse cCP and 3UNF for mouse iCP) revealed[14] that the S1 pocket of subunit β5i is larger than that of β5c (upper row of images). This difference in size was attributed to distinct conformations of Met45 (in green). By contrast, the S3 pocket of β5i is smaller compared to β5c due to Ser27 (in magenta), which in β5c is substituted for Ala. These structural differences served as the starting point for the design of β5c-specific ligands as described here.

the basis of these observations, we created a series of peptide epoxyketone inhibitors varying in size at P1 and in this way identified **52**, which has an improved selectivity (though at the cost of a slightly lowered activity) for β5i over β5c when compared to **51**[15] as well as PR-924,[15a,16] another β5i-selective compound. With the aim to identify β5c selective compounds, we synthesized the hydrophobic tri- and tetrapeptide epoxyketones **1**−**30** (Table 1 and Supporting Information, Table S1) that feature, either a leucine (**1**−**24**) or an alanine (**25**−**30**) at the P1 position, a phenylalanine or methyltyrosine at P2, and an azidophenylalanine or a morpholine at P4. A variety of bulky, aromatic, and aliphatic amino acids were installed at P3 with the aim to identify compounds that still would fit in the more spacious S3 site of β5c but not the S3 site of β5i. The focused compound library was prepared according to our synthetic methodology[11b,17] entailing the synthesis of leucine and alanine epoxyketone as well as solution-phase assembly of the peptide epoxyketones from the corresponding alpha-amino acids (see Experimental Section and Supporting Information). Cyclohexyl-homoalanine (in **15**), methylcyclohexylalanine (in **16**), methoxycyclohexylalanine (in **17**), the decaline-alanines (in **18** and **19**),[18] and bis-cyclohexylalanine (in **20**, **29** and **30**) were prepared from the corresponding aromatic amino acids by hydrogenation in the presence of 5% rhodium on activated alumina (see, for example, the transformation of **31** to **32** (Scheme 1 and Supporting Information)).[19]

Amino acids with chiral carbons emerging after hydrogenolysis were obtained as stereoisomeric mixtures, incorpo-

DOI: 10.1021/acs.jmedchem.6b00705
J. Med. Chem. 2016, 59, 7177−7187

Table 1. Chemical Structures of Compounds 1−30 with Their Respective Inhibitory Activity against β5c and β5i[a]

Compound	R_4	R_3	R_2	R_1	Apparent IC_{50} (nM) β5i	β5c	Ratio β5i/β5c
1					>10	<10	n.d*
2					<10	<10	n.d
3					<10	<10	n.d
4					<10	<10	n.d*
5					<10	<10	n.d
6					<10	<10	n.d*
7					<10	<10	n.d*
8					<10	<10	n.d*
9					<10	<10	n.d*
10					<10	<10	n.d*
11					<10	<10	n.d*
12					<10	<10	n.d*
13					72	33	2
14					50	<10	>5
15					35	36	1
16					18	<10	>2
17					31	<10	>3
18					15	<10	>1.5*
19					25	<10	>2.5*
20					1230	19	65
21					33	<10	>3*
22					68	18	4
23					274	119	2
24					638	853	1
25				H	>10000	>10000	n.d.
26				H	>10000	57	>175
27				H	134	<10	>13
28				H	>10000	853	>12
29				H	>10000	33	>303
30				H	>10000	1230	>8

[a]High β5i/β5c ratio indicates selectivity for β5c. n.d. not determined. *: At 0.01 μM final concentration of **1**, 56% of β5i activity and 44% of β5c remained. Values for compound **4** at 0.01 μM final concentration, 15% β5i activity and 6% β5c activity; for **6**, 49% β5i and 16% β5c; for **7**, 28% β5i and 12% β5c; for **8**, 49% β5i and 14% β5c; for **9**, 28% β5i and 9% β5c; for **10**, 36% β5i and 30% β5c; for **11**, 23% β5i and 9% β5c; for **12**, 44% β5i and 23% β5c; for **18**, 40% β5c; for **19**, 36% β5c; and for **21**, 24% β5c.

Scheme 1[a]

[a]Reagents and conditions: (a) Rh/Al, H_2, MeOH/HCl (1 M, aq) 30:1, then Boc_2O, TEA, THF, H_2O.

rated in the peptide epoxyketones as such and the resulting diastereomers tested as mixtures. All compounds were evaluated on their proteasome inhibition profile in extracts from Raji cells (a human B-cell lymphoma cell line that expresses both cCPs and iCPs) applying our established ABPP assay.[12] Compounds were tested at 0.01, 0.1, 1.0, and 10.0 μM final concentrations, resulting in distinct IC_{50} values as summarized in Table 1.

Compounds **1**−**12**, all featuring a P1-leucine and an aromatic residue at P3, are low nanomolar inhibitors of both β5c and β5i. Discrimination between the two chymotryptic sites starts to emerge within the compound series **13**−**24** with a leucine at P1 and an aliphatic, bulky moiety at P3. Whereas adamantylalanine at P3 (**24**) is detrimental for both β5c and β5i inhibition, all other bulky aliphatic P3-groups appear less well accommodated by β5i than β5c. This effect is most pronounced in bis-cyclohexylalanine derivative **20**, with an apparent IC_{50} for β5i of 1230 nM and for β5c of 19 nM. While the presence of this steric residue decreased β5c inhibition slightly, it is much more

DOI: 10.1021/acs.jmedchem.6b00705
J. Med. Chem. 2016, 59, 7177−7187

Table 2. Apparent IC_{50} (μM) and pIC_{50} Values of Compounds 2, 3, 5, 16, 17, 20, and 29 against the Six Catalytic Sites from Human cCPs and iCPs

	apparent IC_{50} (μM) and pIC_{50} values											
	β5c		β5i		β2c		β2i		β1c		β1i	
compd	IC_{50}	pIC_{50}	IC_{50}	pIC_{50}	IC_{50}	pIC_{50}	IC_{50}	pIC_{50}	IC_{50}	pIC_{50}	IC_{50}	pIC_{50}
2	0.0021	8.67 ± 0.06	0.0055	8.26 ± 0.08	0.067	7.18 ± 0.08	0.013	7.89 ± 0.10	>100	<4.0	0.12	6.91 ± 0.08
3	0.003	8.53 ± 0.06	0.0051	8.29 ± 0.06	0.060	7.22 ± 0.06	0.045	7.34 ± 0.12	>100	<4.0	0.16	6.79 ± 0.12
5	0.0021	8.68 ± 0.04	00078	8.11 ± 0.08	0.11	6.95 ± 0.10	0.029	7.54 ± 0.09	0.18	6.75 ± 0.22	0.13	6.88 ± 0.13
16	0.002	8.70 ± 0.09	0.011	7.96 ± 0.12	0.046	7.34 ± 0.15	0.045	7.35 ± 0.15	>100	<4.0	>100	<4.0
17	0.0021	8.68 ± 0.10	0.022	7.67 ± 0.09	0.066	7.18 ± 0.11	0.063	7.20 ± 0.14	>100	<4.0	0.89	6.05 ± 0.28
20	0.017	7.77 ± 0.07	0.439	6.36 ± 0.17	>100	<4.0	>100	<4.0	>100	<4.0	>100	<4.0
29	0.0747	7.13 ± 0.12	16.7	4.78 ± 0.13	>100	<4.0	>100	<4.0	>100	<4.0	>100	<4.0

severe for β5i, thus introducing a superb possibility to achieve specificity. This discrimination further increases when going from leucine to alanine at P1, as in **29** (which we designated as LU-005c, Figure 1), implementing a β5i/β5c ratio of over 2 orders of magnitude, while having an IC_{50} value of 33 nM for β5c.

To establish the IC_{50} values more accurately and also to obtain insights into the coinhibition of the β1c/β1i/β2c/β2i activities, we selected 6 compounds (**2**, **3**, **5**, **16**, **17**, and **20**) and tested these together with **29** in our competitive ABPP assay using Raji cell extracts at a wider range of final concentrations (Table 2 and Figure S3). The obtained results agree with the trend from our initial screen (Table 1 and Figure S2) and allow us to draw structure−activity relationships. Compounds **2**, **3**, **5**, **16**, **17**, and **20** all inhibit both β5c and β5i at low nanomolar concentrations, and most are cross-reactive toward β2c and β2i (Table 2). Increasing the size at P3 from Phe (**2**) to homo-Phe (**3**) shows similar inhibition profiles, coinhibiting β1i. Further increasing the bulk to a methyl-cyclohexyl-alanine (**16**) results in loss of β1i activity, yielding a compound highly active against the β2c/β2i/β5c/β5i catalytic subunits. Increasing the bulk to bis-cyclohexylalanine (**20**) abolishes activity against β2c/β2i and leads to an inhibitor with considerable specificity for β5c over β5i. Compound **29** differs from **20** in that the P1 site features the alanine side chain, as opposed to leucine. This modification led to the desired β5c specificity.

Having identified the P1-Ala/P3-bis-cyclohexyl-Ala (with Phe at P2) as the optimal sequence for β5c selectivity, we decided to establish which of the two stereoisomers (*cis* or *trans* with respect to the 1,4-disubstituted inner cyclohexane ring) present in compound **29** is the most potent and most selective. For this, we designed a route of synthesis that would deliver both diastereomers of 1,4-bis-cyclohexyl-L-alanine **32** (Scheme 1) in enantiomerically pure form.

The synthesis of *trans*-biscyclohexyl-L-alanine **43** is depicted in Scheme 2 and commences with hydrolysis of α,β-unsaturated nitrile **33**, prepared according to the published procedure,[19] to the corresponding carboxylate, which was esterified to give ethyl ester **34** (79% yield, two steps). Hydrogenolysis of the alkene in **34** (H_2, Pd/C) followed by saponification of the ethyl ester gave the diastereomeric mixture of *trans*- and *cis*-1,4-disubstituted cyclohexanes **35** and **36**, which was separated by silica gel flash column chromatography to provide **35** and **36** in yields of 29% and 28%, respectively. The carboxylic acid in the *trans* isomer **35** was reduced to the primary alcohol, which in two steps (*O*-tosylation followed by treatment with sodium cyanide, 76% yield, three steps) afforded nitrile **37**. Hydrolysis of the nitrile and condensation of the resulting acid with *N*,*O*-dimethylhydroxylamine yielded Weinreb amide **38** (96% yield), which was reduced to the aldehyde and *in situ* subjected to transamination with sulfinamide[20] **40** to provide sulfinimine **39**. In the key step of the sequence, compound **39** was treated with Et_2AlCN in a mixture of *i*-PrOH and THF to give, in an asymmetric Strecker reaction, in good enantiomeric excess cyanide **41** (de ≥96%). The stereoselectivity obtained in the asymmetric Strecker reaction matches those observed by Cordi and co-workers, who first reported[21] the use of *S*-sulfinamides

Scheme 2[a]

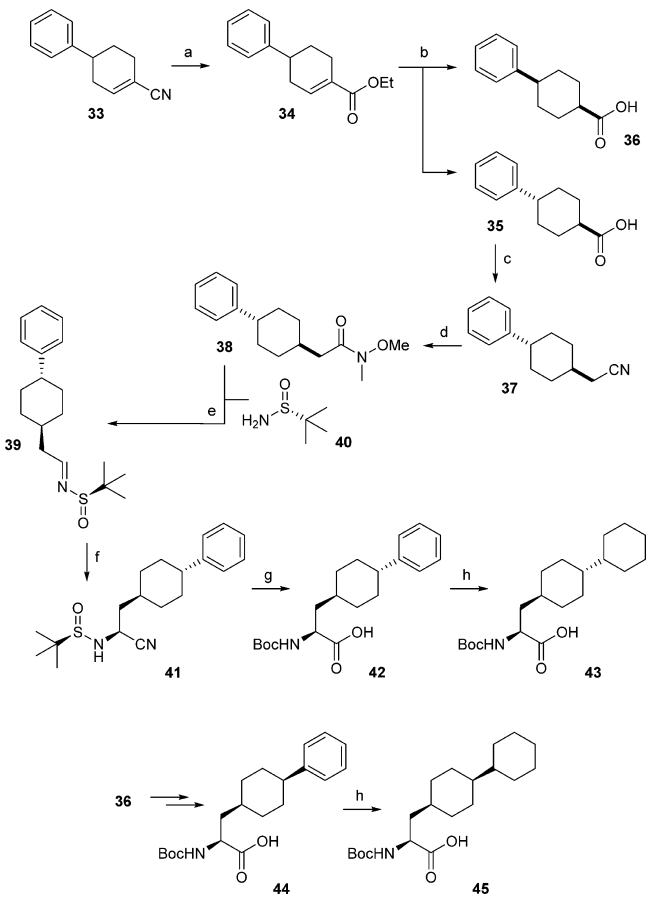

[a]Reagents and conditions: (a) (i) 2M NaOH; (ii) C_2H_5OH, conc. H_2SO_4; (b) (i) Pd/C, C_2H_5OH, H_2; (ii) NaOH; (iii) silica gel column chromatography; (c) (i) $LiAlH_4/Et_2O$; (ii) TsCl/TEA/DCM; (iii) NaCN/DMF; (d) (i) KOH/ethylene glycol; (ii) *N*,*O*-dimethylhydroxylamine hydrochloride, HCTU/DiPEA/DCM; (e) (i) $LiAlH_4/Et_2O$; (ii) **40**/$CuSO_4$/DCM; (f) Et_2AlCN/*i*-PrOH/THF; (g) (i) 6M HCl, reflux; (ii) Boc_2O/TEA/THF/H_2O; (h) Rh/Al, H_2/MeOH.

DOI: 10.1021/acs.jmedchem.6b00705
J. Med. Chem. 2016, 59, 7177−7187

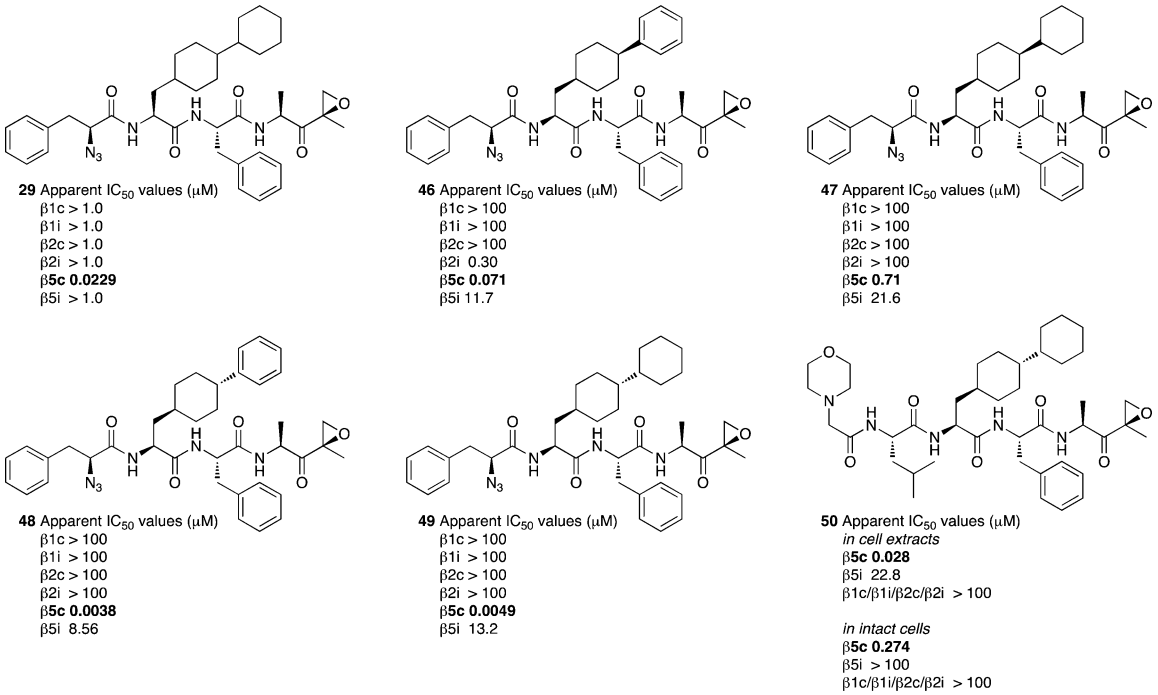

Figure 3. Apparent IC_{50} values of compounds **29** and **46**–**50** against the six catalytic sites from human cCPs and iCPs.

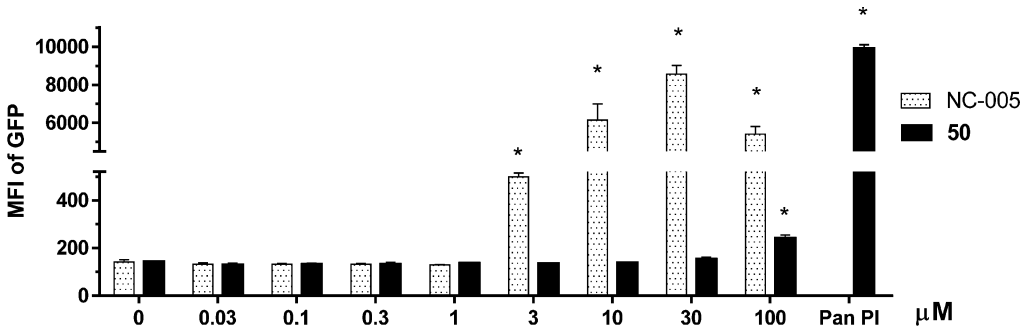

Figure 4. AMO-1 multiple myeloma cells expressing Ub-GFP were treated with indicated concentrations of compound **50** and β5c/β5i selective inhibitor NC-005 for 1 h, washed with PBS, and cultivated for an additional 12 h in medium before measuring the median fluorescence intensity (MFI) of GFP. Complete proteasome inhibition (PanPI) can be achieved by combining 5 μM NC-005 (β5c/β5i), 5 μM NC-001 (β1c/β1i), and 3 μM LU-102 (β2c/β2i).

in this reaction and observed the predominant formation of S-configured products as well. Hydrolysis of the cyanide to the carboxylate and the sulfinamide to the amine, and ensuing N-Boc protection afforded *trans*-4-phenyl-L-cyclohexylalanine **42** (47% over the three steps). Hydrogenation of the phenyl moiety in **42** to the corresponding cyclohexyl (**43**, H_2, Ru/Al, quantitative yield) concluded the synthesis scheme. In a similar fashion and efficiency, *cis*-1,4-disubstituted cyclohexane **36** was transformed into the corresponding cyclohexylalanine derivatives **44** and **45** (see Supporting Information for details).

The diastereomeric cyclohexylalanine derivatives **43** and **45**, as well as their unsaturated precursors **42** and **44**, were introduced at P3 of the N_3-Phe-X-Phe-Ala-epoxyketone (EK) sequence to yield the four structurally closely related peptide epoxyketones **46**–**49** (Figure 3). These compounds were subjected to our competitive ABPP assay and the results compared to the data obtained for the diastereomeric mixture of compounds **29** (Figure 3, Figure S4 and Table S2). All four compounds proved to be potent and selective β5c inhibitors. As can be seen, the *trans*-substituted derivatives **48** and **49** are both the most potent and the most selective inhibitors of the series (**48**, β5i/β5c = 2253; **49**, β5i/β5c = 2694; in comparison, **46**, β5i/β5c = 165; **47**, β5i/β5c = 30). When we assessed compound **49** in living RPMI-8226 cells though, no proteasome inhibition was observed. Likely, compound **49** is too hydrophobic to cross the cell membrane. The same probably applies to the stereoisomers of **49** (**46**, **47**, and **48**), which we did not evaluate but which are equally apolar. To overcome this shortcoming (and as we had done for the mixture of diastereomers **29** in our previous report[12]), we substituted the azidoPhe N-terminal cap in **49** for the morpholinoacetyl-Leu cap to obtain the peptide epoxyketone **50**. Though compound **50** is slightly less potent (IC_{50} for β5c 28 nM), it still possesses significant selectivity (β5i/β5c = 814) and inhibits β5c in RPMI-8226 cells with an IC_{50} for β5c of 274 nM, whereas the IC_{50} values for all other subunits are above 100 μM (Figure S5 and Tables S2, S3).

Further evaluation of compound **50** was performed on AMO-1 multiple myeloma cells expressing ubiquitinated green fluorescent protein (Ub-GFP).[22] This tool allows direct

DOI: 10.1021/acs.jmedchem.6b00705
J. Med. Chem. 2016, 59, 7177–7187

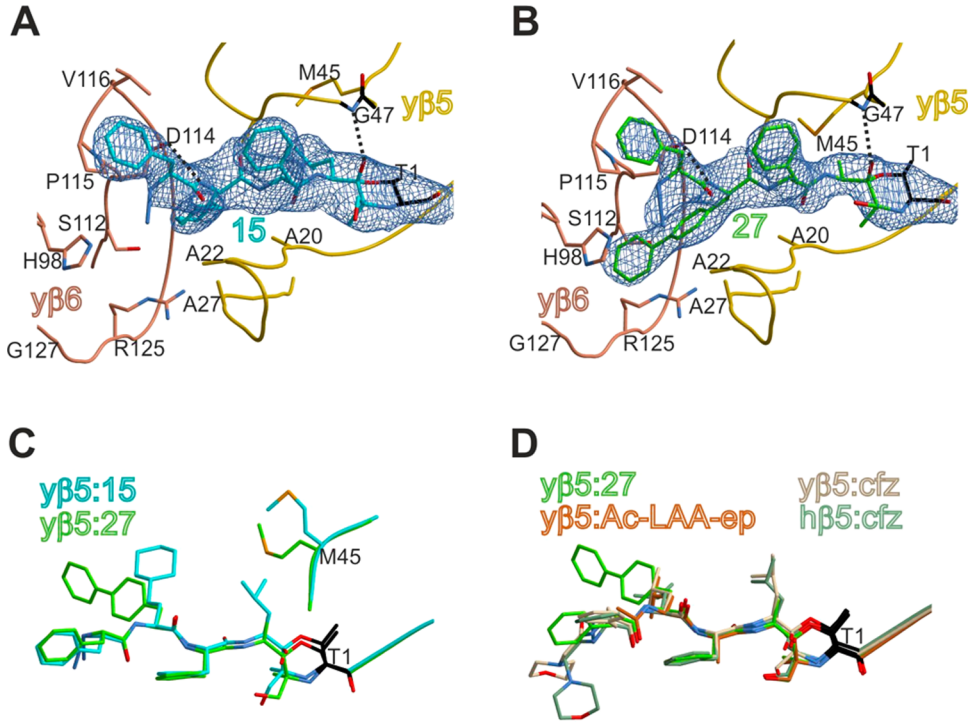

Figure 5. Yeast 20S proteasomes in complex with the epoxyketones **15** (PDB code: 5JHS) and **27** (PDB code: 5JHR). (A,B) Compound **15** (A) and compound **27** (B) bound to the yβ5/yβ6 active site. The $2F_O - F_C$ electron density map for the ligand and Thr1 (black) is shown as a blue mesh contoured at 1σ. Hydrogen bonds are indicated by black dotted lines. Amino acids are labeled by the one-letter code and numbered according to the sequence alignment to the proteasomal β subunit of *Thermoplasma acidophilum*. (C) Structural superposition of the compounds **15** and **27** bound to subunit yβ5. In contrast to **15**, binding of **27** does not trigger conformational changes of the Met45 side chain. (D) Structural superposition of the ligands **27**, Ac-LAA-EK, and carfilzomib bound to either yβ5 or the human constitutive β5c subunit depicts their identical binding modes.

assessment of the accumulation of polyubiquitinated proteasome substrate proteins upon functional proteasome inhibition. We observed that, although β5c is effectively inhibited, this does not result in Ub-GFP accumulation (Figure 4). Presumably, β5i, either alone or in combination with other unaffected catalytic sites, compensates for the loss of β5c activity in the turnover of Ub-GFP. The ability of different proteasomal subunits to compensate for one nonfunctional subunit has been shown previously.[23] At 100 μM final concentration of compound **50**, β5i is partially coinhibited, and this leads to an increase in GFP-mediated fluorescence. In comparison, the β5c/β5i selective inhibitor, NC-005,[24] causes accumulation of Ub-GFP at 3 μM. The maximal level of Ub-GFP accumulation was established by complete inhibition of all proteasome activities using a combination of NC-005 (blocking β5c/β5i), NC-001[24] (blocking β1c/β1i) and LU-102[25] (blocking β2c/ β2i; Figure S6). Compound **50** has an *in situ* proteasome inhibition profile in AMO-1 Ub-GFP cells similar to that observed in RPMI-8226 cells (see Figure S7−10), and inhibitor concentrations used in the Ub-GFP accumulation experiments were based on this observation.

With the aim to gain insight into the observed subunit specificities, we set out to obtain crystal structures of the most potent compounds complexed to proteasomes. Crystal soakings were only successful for compounds **15** (P3 homocyclohexylalanine; P1 leucine) and **27** (P3 biphenylalanine; P1 alanine) (Tables S4 and S5). Because of their high hydrophobicity, most compounds precipitated under the crystallization condition of the yeast 20S proteasome core particle (yCP). Notably, in contrast to inhibition assays that use only low concentrations of protein and inhibitor, the crystal drop is set up with a proteasome concentration of 40 mg/mL and requires millimolar ranges of ligands to achieve full occupancy of the compounds at the active sites.

The obtained crystal structure of compound **15** shows that the P3-cyclohexyl-homoalanine residue of the ligand protrudes deeply into the S3 pocket of the yβ5/yβ6 substrate binding channel and undergoes hydrophobic interactions with the amino acid side chains of Ala20, Ala27, and Val31 of yβ5 as well as the hydrophobic atoms of the side chain of Asp114 and Glu120 of subunit yβ6 (Figure 5A). The P1-Leu moiety, known to be suitable for β5i and β5c, likely causes the observed nonselectivity of **15** between β5i and β5c (Table 1). Substituting the P3-cyclohexyl-homoalanine residue of **15** for a bis-cyclohexylalanine derivative (**20**) significantly increases β5c-selectivity (by a factor of 65). Most likely, Ser27 (β5i) shaping the S3 pocket of the β5i/β6 substrate binding channel, sterically hinders binding of the hydrophobic bis-cyclohexyl-homoalanine, while Ala27 (β5c) favors the interaction with this P-site, thereby promoting β5c-inhibition. In agreement with this, compound **20** is 35 times less active toward β5i than compound **15** but slightly more potent for β5c (1.9 fold; Table 1). Substitution of the P1-Leu residue of inhibitor **20** for a P1-Ala residue yields compound **29**, a very potent β5c-selective inhibitor. Because of its insolubility, we could not determine a crystal structure of **29**; however, structural data could be obtained on **27**, a derivative of **29** featuring a P3-biphenyl moiety instead of the saturated bis-cyclohexyl-homoalanine (Figure 5B). The P3-biphenyl moiety of **27** adopts a different conformation than the cyclohexyl-homoalanine of **15** and occupies a distinct well-defined cavity at the interface of the subunits yβ5 and yβ6. Ile100 and Gly127 of subunit yβ6 form

DOI: 10.1021/acs.jmedchem.6b00705
J. Med. Chem. 2016, 59, 7177−7187

the bottom of this pocket, while His98 and Arg125 laterally restrict it. Additional hydrophobic interactions are provided by Ala27 of yβ5 and the hydrophobic atoms of the side chain of Asp114 (yβ6). Notably, the chemical character of the interacting yβ6 residues is conserved in mouse and human β6 (Figures 5B, S11A and S11B). As previously noted for Ac-LAA-EK,[11b] the P1-Ala residue of **27** does not change the conformation of Met45 (Figure 5C). Structural superpositions of **27** with Ac-LAA-EK as well as carfilzomib bound to subunit β5 of yeast[26] and human proteasomes[27] reveal that the ligands' P1 and P2 residues align well, whereas the P3 sites and the N-caps are more variable in their conformation (Figure 5D). Altogether, the obtained structural data suggest that the overall binding mode of β5c selective ligands like Ac-LAA-EK and **27** is similar to that of nonselective compounds like **15** and carfilzomib. Thus, selectivity for either β5i or β5c is mainly gained by shape complementarity of the P1 and P3 residues with the S1 and S3 pockets, respectively.

DISCUSSION AND CONCLUSIONS

This work describes the development and evaluation of a set of potent and highly selective inhibitors of the β5c catalytic activity of human proteasomes. As we did before in our work on β5i- and β1i-specific inhibitors,[13] we sought to achieve selectivity, not so much by optimizing affinity for the target subunit as by introducing penalties for the most closely related subunits, here β5i. The most selective compound in the described series, compound **49**, inhibits β5c in the nanomolar range and over 3 orders of magnitude more potently than β5i. The most prominent distinguishing feature in **49** is its P3 substituent, being a steric bis-cyclohexylalanine residue. In our previous work,[12] we introduced this residue as a mixture of stereoisomers. Here, we describe a stereoselective synthesis of both enantiomers, which proceeds through their partially unsaturated analogues. The route of synthesis we employed, making use of Strecker chemistry starting from chiral sulfinimines, along with the synthesis of the four structurally related amino acids **42**−**45**, may be of relevance for the construction of peptide-based materials other than those reported in the present work. The crystallographical insights confirm our design, which we based on the murine cCP and iCP structures and the notion that β5c would prefer a large P3 residue accompanied by a small P1 residue.[14] Furthermore, modeling based on the structural data indicates that the P3-*trans*-bis-cyclohexylalanine residues of compounds **48** and **49** bind in the energetically favored chair conformation, while the less potent P3-*cis*-analogues (compounds **46** and **47**) adopt the twist-boat form with higher energy.

Compound **49** appeared not able to reach proteasomes within living cells, and we attribute this to the fact that the molecule is too hydrophobic. With the aim to create a cell-permeable analogue, we substituted the N-terminal indene cap in **49** for a morpholino-leucine, arriving at compound **50**. Though this agent turned out to be somewhat less active and selective, it is cell permeable. Therefore, compound **50** is the most effective compound described to date for specific chemical knock down of β5c in cells. We demonstrate that selective inhibition of β5c in Ub-GFP-transfected AMO-1 cells (a multiple myeloma cell line expressing cCPs and iCPs in about equal amounts) did not lead to accumulation of the fluorescent proteasome substrate. This result underscores the findings in literature that inhibition of β5c alone is not sufficient to cause cell death.[28] In conclusion, we believe that our set of β5c inhibitors will become a highly valuable tool for fundamental and applied biological as well as biomedical research on proteasomes in relation to oncology and immunology. The β5c-selective inhibitors reported here may assist in the establishment of the optimal cCP/iCP subunit inhibition regime, in cell lines and specifically also in primary tumors, and with the aim to improve the therapeutic window. Furthermore, our β5c selective inhibitors may be of use in the assessment, in a chemical ligandomics approach, of the contribution of β5c to the production of MHCI peptide repertoires.

EXPERIMENTAL SECTION

General Procedures. All reagents were of commercial grade and used as received unless indicated otherwise. The purity of all tested compounds is >95% on the basis of LC-MS and NMR. ^{1}H and ^{13}C NMR spectra were recorded on a Bruker AV-400 (400 MHz), AV-600 (600 MHz), or AV-850 (850 MHz) spectrometer. Chemical shifts are given in ppm (δ) relative to CD_3OD or $CDCl_3$ as the internal standard. Coupling constants are given in Hz, and peak assignments are based on 2D ^{1}H COSY and ^{13}C HSQC NMR experiments. All presented ^{13}C APT spectra are proton decoupled. LC-MS analysis was performed on a Finnigan Surveyor HPLC system with a Gemini C18 50 × 4.60 mm column (detection at 200−600 nm) coupled to a Finnigan LCQ Advantage Max mass spectrometer with ESI. Methods used are 15 min (0−0.5 min, 10% MeCN; 0.5−10.5 min, 10% to 90% MeCN; 10.5−12.5 min, 90% MeCN; 12.5−15 min, 90% to 10% MeCN) or 12.5 min (0−0.5 min, 10% MeCN; 0.5−8.5 min, 10% to 90% MeCN; 8.5−10.5 min, 90% MeCN; 10.5−12.5 min, 90% to 10% MeCN). HRMS was recorded on a LTQ Orbitrap (ThermoFinnigan). For reverse phase HPLC purification, an automated Gilson HPLC system equipped with a C18 semiprep column (Phenomenex Gemini C18, 5 μm 250 × 10 mm) and a GX281 fraction collector was used.

General Procedure for Azide Couplings. Compounds **1**−**30** and **46**−**50** were prepared via azide coupling of properly protected tripeptide hydrazide and properly deprotected Leu epoxyketone amines and Ala epoxyketone amines. The appropriate hydrazide was dissolved in 1:1 DMF/DCM (v/v) and cooled to −30 °C. *t*BuONO (1.1 equiv) and HCl (4N solution in 1,4-dioxane, 2.8 equiv) were added, and the mixture was stirred for 3 h at −30 °C after which TLC analysis (10% MeOH/DCM, v/v) showed complete consumption of the starting material. The epoxyketone was added as a free amine to the reaction mixture as a solution in DMF with 5.0 equiv of DiPEA. The mixture was allowed to warm to r.t. slowly overnight. The mixture was diluted with EtOAc and extracted with H_2O (3×) and brine. The organic layer was dried over $MgSO_4$ and purified by flash column chromatography (1−5% MeOH in DCM) or reverse phase HPLC. Peptide hydrazides were prepared by hydrazinolysis of peptide methyl esters synthesized by standard procedures of solution peptide chemistry as described in the Supporting Information.

*N_3Phe-BiCha-Phe-Leu-EK (**20**).* The tripeptide hydrazide N_3Phe-BiCha-Phe-$NHNH_2$ was prepared according to literature procedures,[12] and the title compound was prepared according to the general procedure for azide coupling on a 50 μmol scale. Purification by HPLC (85%−100% MeCN-H_2O) yielded the title compound (7.5 mg, 10.3 μmol, 21%). ^{1}H NMR (600 MHz, MeOD) δ 7.38−7.09 (m, 10H), 4.66−4.62 (m, 1H), 4.57−4.54 (m, 1H), 4.44−4.36 (m, 1H), 4.10−4.07 (m, 1H), 3.23 (t, J = 4.5 Hz, 1H), 3.14−3.10 (m, 2H), 3.00−2.83 (m, 3H), 1.84−1.64 (m, 8H), 1.52−0.88 (m, 27H). ^{13}C NMR (150 MHz, MeOD) δ 209.33, 209.31, 173.92, 173.88, 173.19, 173.17, 171.45, 171.39, 138.22, 138.20, 137.89, 137.84, 130.43, 130.42, 130.40, 129.61, 129.59, 129.42, 128.02, 127.72, 65.40, 59.99, 59.98, 55.50, 52.97, 52.94, 52.56, 51.44, 44.75, 44.67, 40.51, 40.41, 40.37, 38.81, 38.75, 38.69, 38.66, 35.49, 34.93, 33.73, 31.70, 31.44, 31.23, 30.93, 30.79, 29.40, 27.96, 27.89, 27.87, 26.64, 26.35, 26.23, 23.79, 21.62, 16.94. LC-MS (linear gradient 10 → 90% MeCN/H_2O, 0.1% TFA, 12.5 min). R_t (min): 11.43 (ESI-MS (m/z): 727.33, (M + H$^+$)).

DOI: 10.1021/acs.jmedchem.6b00705
J. Med. Chem. 2016, 59, 7177−7187

HRMS calculated for $C_{42}H_{58}N_6O_5$ 727.45415 $[M + H]^+$; found 727.45465.

*N_3Phe-cis-Cha(4-Phe)-Phe-Ala-EK (**46**).* The title compound was prepared according to the general procedure for azide coupling on a 50 μmol scale. Purification by HPLC (70%−85% MeCN-H_2O) yielded the title compound (6.9 mg, 10.2 μmol, 20%). ^{1}H NMR (400 MHz, $CDCl_3$) δ 7.37−7.13 (m, 17H), 6.71 (d, *J* = 7.7 Hz, 1H), 6.52 (d, *J* = 7.9 Hz, 1H), 6.39 (d, *J* = 7.0 Hz, 1H), 4.61 (q, *J* = 7.2 Hz, 1H), 4.52−4.45 (m, 1H), 4.32−4.26 (m, 1H), 4.13−4.10 (m, 1H), 3.30−3.26 (m, 1H), 3.17 (d, *J* = 5.0 Hz, 1H), 3.10−3.00 (m, 3H), 2.89 (d, *J* = 4.9 Hz, 1H), 2.56−2.50 (m, 1H), 1.97−1.82 (m, 1H), 1.68−1.39 (m, 14H), 1.24 (d, *J* = 7.0 Hz, 3H). ^{13}C NMR (100 MHz, $CDCl_3$) δ 207.82, 171.36, 170.13, 168.86, 147.05, 136.48, 135.79, 129.68, 129.41, 128.81, 128.75, 128.44, 127.47, 127.19, 127.00, 126.02, 65.16, 59.02, 54.31, 52.54, 51.83, 48.18, 43.44, 38.31, 37.94, 33.60, 30.61, 29.43, 29.16, 28.87, 28.61, 17.32, 16.92. LC-MS (linear gradient 10 → 90% MeCN/H_2O, 0.1% TFA, 12.5 min). R_t (min): 9.40 (ESI-MS (*m*/*z*): 678.93, $(M+H^+)$). HRMS calculated for $C_{39}H_{46}N_6O_5$ 679.36025 $[M + H]^+$; found 679.36047.

*N_3Phe-cis-BiCha-Phe-Ala-EK (**47**).* This compound was prepared according to the general procedure for azide coupling on a 50 μmol scale. Purification by HPLC (70%−85% MeCN-H_2O) yielded the title compound (16.1 mg, 23.5 μmol, 47%). ^{1}H NMR (400 MHz, $CDCl_3$) δ 7.35−7.13 (m, 10H), 6.66 (d, *J* = 7.7 Hz, 1H), 6.50 (d, *J* = 7.8 Hz, 1H), 6.39 (d, *J* = 7.0 Hz, 1H), 4.63−4.57 (m, 1H), 4.51−4.44 (m, 1H), 4.29−4.23 (m, 1H), 4.10−4.07 (m, 1H), 3.27 (dd, *J* = 14.1, 4.1 Hz, 1H), 3.17 (d, *J* = 4.0 Hz, 1H), 3.10−2.93 (m, 3H), 2.89 (d, *J* = 4.9 Hz, 1H), 1.77−1.62 (m, 6H), 1.51 (s, 3H), 1.42−1.01 (m, 18H), 0.94−0.76 (m, 2H). ^{13}C NMR (100 MHz, $CDCl_3$) δ 207.66, 171.33, 170.03, 168.70, 136.36, 135.73, 129.50, 129.28, 128.68, 128.60, 127.32, 127.03, 65.05, 58.88, 54.12, 52.40, 51.60, 48.01, 41.65, 40.42, 38.23, 37.80, 34.85, 30.68, 30.50, 29.89, 28.78, 26.74, 25.37, 25.20, 17.17, 16.78. LC-MS (linear gradient 10 → 90% MeCN/H_2O, 0.1% TFA, 12.5 min). R_t (min): 10.53 (ESI-MS (*m*/*z*): 685.13, $(M+H^+)$). HRMS calculated for $C_{39}H_{52}N_6O_5$ 685.40720 $[M + H]^+$; found 685.40722.

*N_3Phe-trans-Cha(4-Phe)-Phe-Ala-EK (**48**).* This compound was prepared according to the general procedure for azide coupling on a 50 μmol scale. Purification by HPLC (70%−85% MeCN-H_2O) yielded the title compound (5.8 mg, 8.5 μmol, 17%). ^{1}H NMR (850 MHz, $CDCl_3$) δ 7.35−7.27 (m, 7H), 7.26−7.17 (m, 8H), 6.65 (d, *J* = 7.6 Hz, 1H), 6.53 (d, *J* = 7.8 Hz, 1H), 6.35 (d, *J* = 7.0 Hz, 1H), 4.65−4.60 (m, 1H), 4.50−4.47 (m, 1H), 4.37−4.34 (m, 1H), 4.10−4.08 (m, 1H), 3.31−3.28 (m, 1H), 3.16 (d, *J* = 4.9, 1H), 3.07 (d, *J* = 7.1 Hz, 2H), 3.04−3.02 (m, 1H), 2.90 (d, *J* = 4.9 Hz, 1H), 2.44−2.41 (m, 1H), 1.88−1.84 (m, 2H), 1.80−1.73 (m, 2H), 1.67−1.64 (m, 1H), 1.52 (s, 3H), 1.42−1.35 (m, 3H), 1.25 (d, *J* = 7.1 Hz, 3H), 1.10−0.97 (m, 3H). ^{13}C NMR (213 MHz, $CDCl_3$) δ 207.77, 171.37, 170.14, 168.85, 147.40, 136.43, 135.87, 129.65, 129.40, 128.86, 128.78, 128.47, 127.51, 127.22, 126.89, 126.10, 65.18, 59.02, 54.27, 52.54, 51.20, 48.21, 44.28, 38.89, 38.39, 37.98, 34.00, 33.89, 33.72, 32.92, 17.37, 16.93. LC-MS (linear gradient 10 → 90% MeCN/H_2O, 0.1% TFA, 12.5 min). R_t (min): 9.39 (ESI-MS (*m*/*z*): 679.00, $(M+H^+)$). HRMS calculated for $C_{39}H_{46}N_6O_5$ 679.36025 $[M + H]^+$; found 679.36043.

*N_3Phe-trans-BiCha-Phe-Ala-EK (**49**).* This compound was prepared according to the general procedure for azide coupling on a 50 μmol scale. Purification by HPLC (80%−95% MeCN-H_2O) yielded the title compound (11.3 mg, 16.5 μmol, 33%). ^{1}H NMR (400 MHz, $CDCl_3$) δ 7.38−7.11 (m, 10H), 6.64 (d, *J* = 7.7 Hz, 1H), 6.51 (d, *J* = 7.8 Hz, 1H), 6.39 (d, *J* = 7.0 Hz, 1H), 4.66−4.58 (m, 1H), 4.51−4.44 (m, 1H), 4.36−4.30 (m, 1H), 4.13−4.05 (m, 1H), 3.28 (dd, *J* = 14.1, 4.1 Hz, 1H), 3.16 (d, *J* = 4.9 Hz, 1H), 3.09−2.95 (m, 3H), 2.89 (d, *J* = 4.9 Hz, 1H), 1.75−1.56 (m, 9H), 1.51 (s, 3H), 1.38−0.73 (m, 17H). ^{13}C NMR (100 MHz, $CDCl_3$) δ 207.75, 171.46, 170.16, 168.80, 136.50, 135.95, 129.61, 129.40, 128.85, 128.73, 127.48, 127.16, 65.22, 59.00, 54.24, 52.52, 51.29, 48.13, 43.39, 43.27, 39.08, 38.43, 37.99, 34.35, 33.81, 33.00, 30.36, 29.65, 26.98, 17.33, 16.91. LC-MS (linear gradient 10 → 90% MeCN/H_2O, 0.1% TFA, 12.5 min). R_t (min): 10.53 (ESI-MS (*m*/*z*): 685.00, $(M+H^+)$). HRMS calculated for $C_{39}H_{52}N_6O_5$ 685.40720 $[M + H]^+$; found 685.40740.

*Morph-Leu-trans-BiCha-Phe-Ala-EK TFA salt (**50**).* This compound was prepared according to the general procedure for azide coupling on a 50 μmol scale. Purification by HPLC (50%−55% MeCN-H_2O) yielded the title compound (9.9 mg, 11.4 μmol, 23%). ^{1}H NMR (400 MHz, MeOD) δ 7.32−7.15 (m, 5H), 4.62−4.58(m, 1H), 4.49−4.32 (m, 3H), 3.95−3.74 (m, 6H), 3.20 (s, 6H), 2.98−2.82 (m, 2H), 1.82−1.60 (m, 10H), 1.60−1.45 (m, 7H), 1.31−1.11 (m, 7H), 1.08−0.80 (m, 14H). ^{13}C NMR (100 MHz, MeOD) δ 209.33, 174.34, 174.24, 172.76, 138.24, 130.43, 129.38, 127.72, 65.45, 60.00, 55.27, 54.09, 53.25, 53.11, 52.61, 49.09, 49.00, 44.77, 44.65, 41.97, 40.44, 38.84, 35.49, 34.91, 33.64, 31.47, 31.43, 30.99, 30.89, 27.94, 25.94, 23.51, 21.80, 16.98, 16.48. LC-MS (linear gradient 10 → 90% MeCN/H_2O, 0.1% TFA, 15.0 min). R_t (min): 7.30 (ESI-MS (*m*/*z*): 752.6, $(M+H^+)$). HRMS calculated for $C_{42}H_{65}N_5O_7$752.49568 $[M + H]^+$; found 752.49595.

Biological Analysis. *Competitive Activity-Based Protein Profiling Assay in Cell Lysates.* Lysates of Raji cells were prepared by sonication in 3 volumes of lysis buffer containing 50 mM Tris at pH 7.5, 1 mM DTT, 5 mM $MgCl_2$, 250 mM sucrose, 2 mM ATP, and 0.05% (w/v) digitonin. Protein concentration was determined by the Bradford assay. Cell lysates (diluted to 5 μg of total protein in buffer containing 50 mM Tris at pH 7.5, 2 mM DTT, 5 mM $MgCl_2$, 10% (v/v) glycerol, and 2 mM ATP) were exposed to the inhibitors for 1 h at 37 °C prior to incubation with cocktail ABPs for another 1 h, followed by 3 min of boiling with a reducing gel-loading buffer and fractionation on 12.5% SDS−PAGE. In-gel detection of residual proteasome activity was performed in the wet gel slabs directly on a ChemiDoc MP system using Cy2 settings to detect BODIPY(FL)-LU-112, Cy3 settings to detect BODIPY(TMR)-NC-005-VS and Cy5 settings to detect Cy5-NC-001. Intensities of bands were measured by fluorescent densitometry and normalized to the intensity of bands in mock-treated extracts. Average values of three independent experiments were plotted against inhibitor concentrations in GraphPad Prism (in the initial screening (Table 1, Table S1), experiments were conducted once). pIC_{50} values and associated standard deviations were calculated by GraphPad Prism (note that we converted pIC_{50} values to IC_{50} for clarification; however, this method used allows the determination of the standard deviations only from the pIC_{50} values).

Competitive Activity-Based Protein Profiling Assay in Living RPMI-8226 Cells. RPMI-8226 were cultured in RPMI-1640 media supplemented with 10% (v/v) fetal calf serum, GlutaMAX, and penicillin/streptomycin in a 5% CO_2 humidified incubator. 5−8 × 10^5 cells/mL cells was exposed to inhibitors for 1 h at 37 °C. Cells were harvested and washed twice with PBS. Cell pellets were treated with lysis buffer (50 mM Tris at pH 7.5, 2 mM DTT, 5 mM $MgCl_2$, 10% (v/v) glycerol, 2 mM ATP, and 0.05% (w/v) digitonin) on ice for 1 h, followed by centrifugation at 14000 rpm for 15 min. Proteasome inhibition in the obtained cell lysates was determined using the method described above. Intensities of bands were measured by fluorescent densitometry and divided by the intensity of bands in mock-treated extracts. Gels were stained by Coomassie Brilliant Blue, which was used to correct for gel loading differences. Average values of three independent experiments were plotted against inhibitor concentrations. IC_{50} (inhibitor concentrations giving 50% inhibition) values were calculated using GraphPad Prism software.

*Functional Validation of Compound **50** on AMO-1 Multiple Myeloma Cells Expressing Ub-GFP.* The AMO-1 multiple myeloma cell line was maintained in RPMI-1640 medium supplemented with 10% (v/v) fetal calf serum and penicillin/streptomycin (all Sigma, USA). Cells were electroporated using GenePulser II (Biorad, USA) with the Ub-G76 V-GFP plasmid, which was a gift from Nico Dantuma (Addgene plasmid #11941). This insert allows estimating the activity of the proteasome, as GFP is tagged by Ub and thus immediately degraded. However, when the proteasome is inhibited, the GFP substrate accumulates within the cell, and increase of GFP fluorescence can be observed. Cells carrying the plasmid were selected using G418, 500 μg/mL (Gibco,ThermoFisher, USA), and subcloned using MethoCult (StemCell technologies, USA). After selection, positive clones expressing Ub-G76 V-GFP were identified using FACS Canto II (BD Biosciences, USA). Briefly, 5 × 10^5 cells were seeded

DOI: 10.1021/acs.jmedchem.6b00705
J. Med. Chem. 2016, 59, 7177−7187

and treated for 1 h at 37 °C with indicated concentrations of PI (**50**/NC005). Cells were harvested, washed with PBS to remove PI and subsequently cultured in PI-free medium for 12 h under normal culture conditions (37 °C, 5% CO_2). Then, cells were washed in PBS and analyzed on FACS Canto II for MFI in FITC channel. MFI was analyzed in FlowJo software. Upon treatment with 10 nM bortezomib for 1 h (pulse) followed by a 12 h incubation (chase), the clone giving the highest GFP fluorescence was used for further analyses.

Competitive Activity-Based Protein Profiling Assay in Living AMO-1 Ub-GFP Cells. AMO-1 Ub-GFP were cultured in RPMI-1640 media (Sigma-Aldrich, USA) supplemented with 10% (v/v) fetal calf serum (Sigma-Aldrich, USA), penicillin/streptomycin (Gibco/ThermoFisher Scientific, USA), in a 5% CO_2 humidified incubator. 2×10^6 cells/mL cells was exposed to indicated concentrations of proteasome inhibitors for 1 h at 37 °C. Cells were harvested, washed twice with PBS, and lysed with lysis buffer (20 mM Tris-HCl, 10 mM EDTA, 300 mM NaCl, 2% (v/v) Triton-X, 2 nM *N*-ethylmaleimide, Halt-Protease, and Phosphatase Inhibitor Cocktail (ThermoFisher Scientific, USA)) on ice for 10 min, followed by centrifugation at 14000 rpm for 15 min at 4 °C. For the tricolor labeling, protein load was adjusted to 20 μg using the Bradford-assay (Roti-Nanoquant, ROTH, Germany) in 9 μL and a cocktail of ABPs (1 μL) was added to the lysate in indicated final concentrations. The mixture was incubated for 1 h at 37 °C. Subsequently, 4 μL of loading buffer (Biorad, USA) was added and incubated for 2 min at 90 °C. Proteins were separated using SDS−PAGE on 12% precast MOPC gels (NuPAGE Bis-Tris Precast Gels; ThermoFisher Scientific, USA). Pictures of proteasome subunits were acquired by FUSION SOLO-S (Vilber Lourmat, Germany) equipped with fluorescence excitation/emission filters. Data evaluation was performed using Vision software (Vilber Lourmat, Germany).

Crystallographic Analysis. yCP crystals were grown by hanging drop vapor diffusion as previously described.[29] Inhibitor complex structures were obtained by incubating crystals in 5 μL cryobuffer (20 mM magnesium acetate, 100 mM 2-(*N*-morpholino)ethanesulfonic acid, pH 6.8, and 30% (v/v) 2-methyl-2,4-pentanediol) supplemented with 0.5 μL of inhibitor (50 mM in DMSO) for at least 12 h. Diffraction data were collected at the beamline X06SA at the Paul Scherrer Institute, SLS, Villigen, Switzerland (λ = 1.0 Å). Evaluation of reflection intensities and data reduction were performed with the program package XDS.[30] Molecular replacement was carried out with the coordinates of the yeast 20S proteasome (PDB entry code: 5CZ4[31]) by rigid body refinements (REFMAC5[32]). MAIN[33] and COOT[34] were used to build models. Translation/libration/screw (TLS) refinements finally yielded excellent *R* factors as well as r.m.s.d. bond and angle values. The coordinates, proven to have good stereochemistry from the Ramachandran plots, were deposited in the RCSB Protein Data Bank under the accession codes 5JHS (yCP:**15**) and 5JHR (yCP:**27**) (Table S4).

■ ASSOCIATED CONTENT

Supporting Information

The Supporting Information is available free of charge on the ACS Publications website at DOI: 10.1021/acs.jmedchem.6b00705.

Assays of compounds **1**−**30** and **46**−**50** in Raji lysates, pIC_{50} values, and standard errors of all compounds in cell lysates and intact cells, structures of activity-based probes, X-ray data table, complete synthetic details and characterization of all compounds and synthetic intermediates, and NMR spectra and LC-MS traces of compounds **46**, **47**, **48**, **49**, and **50** (PDF)

SMILES data (CSV)

Accession Codes

Structure factors and coordinates were deposited in the RCSB Protein Data Bank under the accession codes: 5JHS (yCP:**15**) and 5JHR (yCP:**27**).

■ AUTHOR INFORMATION

Corresponding Author

*Tel: +31-0-715274307. E-mail: h.s.overkleeft@chem.leidenuniv.nl.

Author Contributions

B.T.X. and G.B. synthesized the compounds under the supervision of G.M. B.T.X. carried out and analyzed the proteasome inhibition assays under the supervision of B.I.F. and with support from M.S. and A.F.K. E.M.H. and M.G. generated the crystal structures. B.A. and C.D. conducted the functional proteasome inhibition assays. B.T.X., E.M.H., M.G., and H.S.O. wrote the manuscript. H.S.O. conceived and supervised the research project.

Notes

The authors declare no competing financial interest.

■ ACKNOWLEDGMENTS

We thank R. Feicht for the purification of yeast 20S proteasomes and the staff of the beamline X06SA at the Paul Scherrer Institute, Swiss Light Source, Villigen (Switzerland) for assistance during data collection. This work was supported by the China Scholarship Council (CSC Ph.D. fellowship, to B.T.X.), The Netherlands Organization for Scientific Research (NWO-CW, TOP-PUNT grant, to H.S.O.), and the Deutsche Forschungsgemeinschaft (DFG, grant GR1861/10-1, to M.G.).

■ ABBREVIATIONS USED

CP, proteasome core particle; cCPs, constitutive proteasome core particles; iCPs, immunoproteasome core particles; tCPs, thymoproteasome core particles; yCP, yeast proteasome core particles; MHCI, major histocompatibility complex class I; ABPP, activity-based protein profiling; EK, epoxyketone; Ub-GFP, ubiquitinated green fluorescent protein; MFI, median fluorescence intensity; PanPI, complete proteasome inhibition; BODIPY, boron-dipyrromethene, (4,4-difluoro-5,7-dimethyl-4-bora-3a,4a-diaza-s-indacene); BiCha, biscyclohexylalanine; N_3Phe, azidophenylalanine; Morph, morphalinoacetyl; Cha(4-Phe), 4-phenyl-cyclohexylalanine; TLS, translation/libration/screw

■ REFERENCES

(1) (a) Rock, K. L.; Gramm, C.; Rothstein, L.; Clark, K.; Stein, R.; Dick, L.; Hwang, D.; Goldberg, A. L. Inhibitors of the proteasome block the degradation of most cell proteins and the generation of peptides presented on MHC class I molecules. *Cell* **1994**, *78*, 761−771. (b) Hershko, A.; Chiechanover, A. The ubiquitin system. *Annu. Rev. Biochem.* **1998**, *67*, 425−479.

(2) Voges, D.; Zwickl, P.; Baumeister, W. The 26s proteasome: a molecular machine designed for controlled proteolysis. *Annu. Rev. Biochem.* **1999**, *68*, 1015−1068.

(3) (a) Kloetzel, P. M.; Ossendorp, F. Proteasome and peptidase function in MHC-class-I-mediated antigen presentation. *Curr. Opin. Immunol.* **2004**, *16* (1), 76−81. (b) Griffin, T. A.; Nandi, D.; Cruz, M.; Fehling, H. J.; Kaer, L. V.; Monaco, J. J.; Colbert, R. A. Immunoproteasome assembly: cooperative incorporation of interferon gamma (IFN-gamma)-inducible subunits. *J. Exp. Med.* **1998**, *187*, 97−104. (c) Groettrup, M.; Kraft, R.; Kostka, S.; Standera, S.; Stohwasser, R.; Kloetzel, P. M. A third interferon-gamma-induced subunit exchange in the 20S proteasome. *Eur. J. Immunol.* **1996**, *26*, 863−869.

(4) Orlowski, M.; Cardozo, C.; Michaud, C. Evidence for the presence of five distinct proteolytic components in the pituitary multicatalytic proteinase complex. Properties of two components cleaving bonds on the carboxyl side of branched chain and small neutral amino acids. *Biochemistry* **1993**, *32*, 1563−1572.

DOI: 10.1021/acs.jmedchem.6b00705
J. Med. Chem. 2016, 59, 7177−7187

(5) Kloetzel, P.-M. Antigen processing by the proteasome. *Nat. Rev. Mol. Cell Biol.* **2001**, *2*, 179−187.
(6) Murata, S.; Sasaki, K.; Kishimoto, T.; Niwa, S.-I.; Hayashi, H.; Takahama, Y.; Tanaka, K. Regulation of CD8+ T cell development by thymus-specific proteasome. *Science* **2007**, *316*, 1349−1353.
(7) (a) Guillaume, N.; Chapiro, J.; Stroobant, V.; Colau, D.; Van Holle, B.; Parvizi, G.; Bousquet-Dubouch, M. P.; Theate, I.; Parmentier, N.; Van den Eynde, N. J. Twp abundant proteasome subtypes that uniquely process some antigens presented by HLA class I molecules. *Proc. Natl. Acad. Sci. U. S. A.* **2010**, *107*, 18599−18604. (b) Klare, N.; Seeger, M.; Janek, K.; Jungblut, P. R.; Dahlmann, B. Intermediate-type 20S proteasome in HeLa cells: "asymmetric" subunit composition, diversity and adaption. *J. Mol. Biol.* **2007**, *373*, 1−10.
(8) (a) Adams, J.; Behnke, M.; Chen, S.; Cruickshank, A. A.; Dick, L. R.; Grenier, L.; Klunder, J. M.; Ma, Y.-T.; Plamondon, L.; Stein, R. L. Potent and selective inhibitors of the proteasome: dipeptidyl boronic acids. *Bioorg. Med. Chem. Lett.* **1998**, *8*, 333−338. (b) Richardson, P. G.; Sonneveld, P.; Schuster, M. W.; Irwin, D.; Stadtmauer, E. A.; Facon, T.; Harousseau, J. L.; Ben-Yehuda, D.; Lonial, S.; Goldschmidt, H.; Reece, D.; San-Miguel, J. F.; Bladé, J.; Boccadoro, M.; Cavenagh, J.; Dalton, W. S.; Boral, A. L.; Esseltine, D. L.; Porter, J. B.; Schenkein, D.; Anderson, K. D. Bortezomib or high-dose dexamethasone for relapsed multiple myeloma. *N. Engl. J. Med.* **2005**, *352*, 2487−2498.
(9) (a) Demo, S. D.; Kirk, C. J.; Aujay, M. A.; Buchholz, T. J.; Dajee, M.; Ho, M. N.; Jiang, J.; Laidig, G. J.; Lewis, E. R.; Parlati, F.; Schenk, K. D.; Smyth, M. S.; Sun, C. M.; Vallon, M. K.; Woo, T. M.; Molineaux, C. J.; Bennett, M. K. Antitumor activity of PR-171, a novel irreversible inhibitor of the proteasome. *Cancer Res.* **2007**, *67*, 6383−6391. (b) O'Connor, O. A.; Stewart, A. K.; Vallone, M.; Molineaux, C. J.; Kunkel, L. A.; Gerecitano, J. F.; Orlowski, R. Z. A phase 1 dose escalation study of the safety and pharmacokinetics of the novel proteasome inhibitor carfilzomib (PR-171) in patients with hematologic malignancies. *Clin. Cancer Res.* **2009**, *15*, 7085−8091.
(10) Kupperman, E.; Lee, E. C.; Cao, Y.; Bannerman, B.; Fitzgerald, M.; Berger, A.; Yu, J.; Yang, Y.; Hales, P.; Bruzzese, F.; Liu, J.; Blank, J.; Garcia, K.; Tsu, C.; Dick, L.; Fleming, P.; Yu, L.; Manfredi, M.; Rolfe, M.; Bolen, J. Evaluation of the proteasome inhibitor MLN9708 in preclinical models of human cancer. *Cancer Res.* **2010**, *70*, 1970−1980.
(11) (a) Huber, E. M.; Groll, M. Inhibitors for the immuno- and constitutive proteasome: current and future trends in drug development. *Angew. Chem., Int. Ed.* **2012**, *51*, 8708−8720. (b) Huber, E. M.; de Bruin, G.; Heinemeyer, W.; Soriano, G. P.; Overkleeft, H. S.; Groll, M. Systematic analyses of substrate preferences of 20S proteasomes using peptidic epoxyketone inhibitors. *J. Am. Chem. Soc.* **2015**, *137*, 7835−7842.
(12) de Bruin, G.; Xin, B.-T.; Kraus, M.; van der Stelt, M.; van der Marel, G. A.; Kisselev, A. F.; Driessen, C.; Florea, B. I.; Overkleeft, H. S. A set of activity-based probes to visualize human (Immuno)-proteasome activities. *Angew. Chem., Int. Ed.* **2016**, *55*, 4199−4206.
(13) de Bruin, G.; Huber, E. M.; Xin, B.-T.; van Rooden, E. J.; Al-Ayed, K.; Kim, K.-B.; Kisselev, A. F.; Driessen, C.; van der Stelt, M.; van der Marel, G. A.; Groll, M.; Overkleeft, H. S. Structure-based design of β1i or β5i specific inhibitors of human immunoproteasomes. *J. Med. Chem.* **2014**, *57*, 6197−6209.
(14) Huber, E. M.; Basler, M.; Schwab, R.; Heinemeyer, W.; Kirk, C. J.; Groettrup, M.; Groll, M. Immuno- and constitutive proteasome crystal structures reveal difference in substrate and inhibitor specificity. *Cell* **2012**, *148*, 727−738.
(15) (a) Shenk, K. D.; Parlati, F.; Zhou, H.-J.; Sylvain, C.; Smyth, M. S.; Bennet, M. K.; Laidig, G. J. Compounds for Enzyme Inhibition. U.S Patent 20070293465, Dec 20, 2007. (b) Muchamuel, T.; Basler, M.; Aujay, M. A.; Suzuki, E.; Kalim, K. W.; Lauer, C.; Sylvain, C.; Ring, E. R.; Shields, J.; Jiang, J.; Shwonek, P.; Parlati, F.; Demo, S. D.; Bennett, M. K.; Kirk, C. J.; Groettrup, M. A selective inhibitor of the immunoproteasome subunit LMP7 blocks cytokine production and attenuates progression of experimental arthritis. *Nat. Med.* **2009**, *15*, 781−787.
(16) (a) Kuhn, D. J.; Hunsucker, S. A.; Chen, Q.; Voorhees, P. M.; Orlowski, M.; Orlowski, R. Z. Targeted inhibition of the immunoproteasome is a potent strategy against models of multiple myeloma that overcomes resistance to conventional drugs and nonspecific proteasome inhibitors. *Blood* **2009**, *113*, 4667−4676. (b) Parlati, F.; Lee, S. J.; Aujay, M.; Suzuki, E.; Levitsky, K.; Lorens, J. B.; Micklem, D. R.; Ruurs, P.; Sylvain, C.; Lu, Y.; Shenk, K. D.; Bennett, M. K. Carfilzomib can induce tumor cell death through selective inhibition of the chymotrypsin-like activity of the proteasome. *Blood* **2009**, *114*, 3439−3447.
(17) Xin, B.-T.; de Bruin, G.; Verdoes, M.; Filippov, D. V.; van der Marel, G. A.; Overkleeft, H. S. Exploring dual electrophiles in peptide-based proteasome inhibitors: carbonyls and epoxides. *Org. Biomol. Chem.* **2014**, *12*, 5710−5718.
(18) Klein, S. I.; Molino, B. F. Antithrombotic Azacycloalkylalkanoyl Peptides and Pseudopeptides. U.S Patent 5866685, Feb 2, 1999.
(19) Leopoldo, M.; Lacivita, E.; Colabufo, N. A.; Contino, M.; Berardi, F.; Perrone, R. First structure-activity relationship study on dopamine D_3 receptor agents with N-[4-(4-arylpiperazin-1-yl)butyl]-acrylcarboxamide structure. *J. Med. Chem.* **2005**, *48*, 7919−7922.
(20) Ellman, J. A. Application of tert-butanesulfinamide in the asymmetric synthesis of amines. *Pure Appl. Chem.* **2009**, *75*, 39−46.
(21) Mabic, S.; Cordi, A. A. Synthesis of enantiomerically pure ethylenediamines from chiral sulfinimines: a new twist to the Strecker reaction. *Tetrahedron* **2001**, *57*, 8861−8866.
(22) Dantuma, N. P.; Lindsten, K.; Glas, R.; Jellne, M.; Masucci, M. G. Short-lived green fluorescent proteins for quantifying ubiquitin/proteasome-dependent proteolysis in living cells. *Nat. Biotechnol.* **2000**, *18*, 538−543.
(23) Kraus, M.; Bader, J.; Geurink, P. P.; Weyburne, E. S.; Mirabella, A. C.; Silzle, T.; Shabaneh, T. B.; van der Linden, W. A.; de Bruin, G.; Haile, S. R.; van Rooden, E.; Appenzeller, C.; Li, N.; Kisselev, A. F.; Overkleeft, H. S.; Driessen, C. The novel β2-selective proteasome inhibitor LU-102 synergizes with bortezomib and carfilzomib to overcome proteasome inhibitor resistance of myeloma cells. *Haematologica* **2015**, *100*, 1350−1360.
(24) Verdoes, M.; Willems, L.; van der Linden, W. A.; Duivenvoorden, B. A.; van der Marel, G. A.; Florea, B. I.; Kisselev, A. F.; Overkleeft, H. S. A panel of subunit-selective activity-based proteasome probes. *Org. Biomol. Chem.* **2010**, *8*, 2719−2727.
(25) Geurink, P. P.; van der Linden, W. A.; Mirabella, A. C.; Gallastegui, N.; de Bruin, G.; Blom, A. E. M.; Voges, M. J.; Mock, E. D.; Florea, B. I.; van der Marel, G. A.; Driessen, C.; van der Stelt, M.; Groll, M.; Overkleeft, H. S.; Kisselev, A. F. Incorporation of non-natural amino acids improves cell permeability and potency of specific inhibitors of proteasome trypsin-like sites. *J. Med. Chem.* **2013**, *56*, 1262−1275.
(26) Huber, E. M.; Heinemeyer, W.; Groll, M. Bortezomib-resistant mutant proteasomes: structural and biochemical evaluation with carfilzomib and ONX 0914. *Structure* **2015**, *23*, 407−417.
(27) Harshbarger, W.; Miller, C.; Diedrich, C.; Sacchettini, J. Crystal structure of the human 20S proteasome in complex with carfilzomib. *Structure* **2015**, *23*, 418−424.
(28) Parlati, F.; Lee, S. J.; Aujay, M.; Suzuki, E.; Levitsky, K.; Loren, J. B.; Micklem, D. R.; Ruurs, P.; Sylvain, C.; Lu, Y.; Shenk, K. D.; Bennett, M. K. Carfilzomib can induce tumor cell death through selective inhibition of the chymotrypsin-like activity of the proteasome. *Blood* **2009**, *114*, 3439−3447.
(29) Gallastegui, N.; Groll, M. Analysing properties of proteasome inhibitors using kinetic and X-ray crystallographic studies. *Methods Mol. Biol.* **2012**, *832*, 373−390.
(30) Kabsch, W. X. D. S. *Acta Crystallogr., Sect. D: Biol. Crystallogr.* **2010**, *66*, 125−132.
(31) Huber, E. M.; Heinemeyer, W.; Li, X.; Arendt, C. S.; Hochstrasser, M.; Groll, M. A unified mechanism for proteolysis and autocatalytic activation in the 20S proteasome. *Nat. Commun.* **2016**, *7*, 10900.
(32) Vagin, A. A.; Steiner, R. A.; Lebedev, A. A.; Potterton, L.; McNicholas, S.; Long, F.; Murshudov, G. N. REFMAC5 dictionary:

DOI: 10.1021/acs.jmedchem.6b00705
J. Med. Chem. 2016, 59, 7177−7187

organization of prior chemical knowledge and guidelines for its use. *Acta Crystallogr., Sect. D: Biol. Crystallogr.* **2004**, *60*, 2184−2195.
(33) Turk, D. MAIN software for density averaging, model building, structure refinement and validation. *Acta Crystallogr., Sect. D: Biol. Crystallogr.* **2013**, *69*, 1342−1357.
(34) Emsley, P.; Lohkamp, B.; Scott, W. G.; Cowtan, K. Features and development of Coot. *Acta Crystallogr., Sect. D: Biol. Crystallogr.* **2010**, *66*, 486−501.

DOI: 10.1021/acs.jmedchem.6b00705
J. Med. Chem. 2016, 59, 7177−7187